JOURNAL OF VIROLOGY, May 2002, p. 4709–4722 Vol. 76, No. 10
0022-538X/02/$04.00+0 DOI: 10.1128/JVI.76.10.4709–4722.2002

Human Immunodeficiency Virus Type 1 Uses Lipid Raft-Colocalized CD4 and Chemokine Receptors for Productive Entry into $CD4^+$ T Cells

Waldemar Popik,* Timothy M. Alce, and Wei-Chun Au

Oncology Center, The Johns Hopkins University School of Medicine, Baltimore, Maryland 21231

Received 16 August 2001/Accepted 8 February 2002

In this report, we describe a crucial role of lipid raft-colocalized receptors in the entry of human immunodeficiency virus type 1 (HIV-1) into $CD4^+$ T cells. We show that biochemically isolated detergent-resistant fractions have characteristics of lipid rafts. Lipid raft integrity was required for productive HIV-1 entry as determined by (i) semiquantitative PCR analysis and (ii) single-cycle infectivity assay using HIV-1 expressing the luciferase reporter gene and pseudotyped with HIV-1 HXB2 envelope or vesicular stomatitis virus envelope glycoprotein (VSV-G). Depletion of plasma membrane cholesterol with *methyl*-β-cyclodextrin (MβCD) relocalized raft-resident markers to a nonraft environment but did not significantly change the surface expression of HIV-1 receptors. MβCD treatment inhibited productive infection of HIV-1 by 95% as determined by luciferase activity in cells infected with HXB2 envelope-pseudotyped virus. In contrast, infection with VSV-G-pseudotyped virus, which enters the cells through an endocytic pathway, was not suppressed. Biochemical fractionation and confocal imaging of HIV-1 receptor distribution in live cells demonstrated that CD4, CCR5, and CXCR4 colocalized with raft-resident markers, ganglioside GM1, and glycosylphosphatidylinositol-anchored CD48. While confocal microscopy analysis revealed that HIV-1 receptors localized most likely to the same lipid microdomains, sucrose gradient analysis of the receptor localization showed that, in contrast to CD4 and CCR5, CXCR4 was associated preferentially with the nonraft membrane fraction. The binding of HIV-1 envelope gp120 to lipid rafts in the presence, but not in the absence, of cholesterol strongly supports our hypothesis that raft-colocalized receptors are directly involved in virus entry. Dramatic changes in lipid raft and HIV-1 receptor redistribution were observed upon binding of HIV-1 NL4-3 to PM1 T cells. Colocalization of CCR5 with GM1 and gp120 upon engagement of CD4 and CXCR4 by HIV-1 further supports our observation that HIV-1 receptors localize to the same lipid rafts in PM1 T cells.

The plasma membrane of eukaryotic cells contains numerous lipid microdomains in a liquid ordered phase floating in the plane of a less ordered membrane environment. The lipids present in microdomains are asymmetrically distributed over the two leaflets in the bilayer. In the exoplasmic leaflet, sphingolipids and cholesterol assemble laterally to form microdomains called lipid rafts (4, 52).

In polarized cells, lipid rafts are concentrated at the apical surface, whereas in nonpolarized cells they are dispersed over the cell surface as small (about 30 to 50 nm in diameter), highly dynamic domains able to include about 10 to 30 protein molecules (44). The raft size can be modulated by oligomerization of raft components; however, the precise mechanism and signals that may lead to raft aggregation are not clear.

Lipid rafts are involved in membrane trafficking, cell morphogenesis, and signal transduction (52, 53). Numerous signaling molecules are concentrated in raft domains, including Src family kinases and heterotrimeric G proteins, as well as molecules involved in Ca^{2+} influx (53). It has been shown that recruitment of the T-cell receptor (TCR) to lipid rafts upon receptor stimulation coincided with the aggregation of lipid rafts and triggering of signaling cascades (22). The functional importance of TCR localization to rafts was confirmed by the observation that disintegration of rafts by cholesterol depletion inhibited receptor tyrosine phosphorylation and signaling in T cells (55).

The mechanisms by which signaling proteins associate with rafts are not well understood. Lipidation of some signaling proteins with saturated acyl chains may play an important role in their preferential localization to membrane rafts. Similarly, the mechanism responsible for targeting of transmembrane proteins and receptors to lipid rafts is unclear. Recently, it has been reported that the transmembrane domains of influenza virus hemagglutinin (49) and neuraminidase provide signals for their association with rafts. In addition, association of transmembrane proteins with rafts may employ direct protein-lipid interactions (49).

Targeting of signaling proteins to rafts may affect their functions in different ways. First, increased concentration of these proteins in rafts may facilitate their intermolecular interactions. Second, the ordered lipid environment may affect functional properties of the receptors (4, 15). An abundance of evidence suggests the existence of distinct types of lipid microdomains, each with specific components (45). For example, microdomains containing caveolin are distinct from other types of microdomains (20). However, neither caveolin proteins nor caveola structures are detected in blood cells.

Although the presence of CD4 (35) and CCR5 (32) in detergent-resistant membrane microdomains has been demon-

* Corresponding author. Mailing address: Oncology Center, The Johns Hopkins University, 1650 Orleans St., Baltimore, MD 21231. Phone: (410) 955-8873. Fax: (410) 955-0840. E-mail: wpopik@jhmi.edu.

strated, the distribution of CD4, CCR5, and CXCR4 receptors in T-cell lipid rafts remains largely unknown. Recent studies, using immunogold electron microscopy, have clearly shown the existence of homogenous microclusters of CD4 and chemokine receptors separated by distances of less than 100 nm, suggesting that these human immunodeficiency virus type 1 (HIV-1) receptors may colocalize in rafts (54).

It has been shown that the assembly and budding of different viruses, including measles virus (33), Semliki Forest virus (30), influenza virus (50), Sindbis virus (31), murine leukemia virus (29), and HIV-1 (18, 36, 38), take place in lipid rafts. Consequently, HIV-1 particles produced by infected T cells have been shown to incorporate raft-resident proteins and glycolipids into the viral envelope (36).

Raft-colocalized receptors may be crucial for entry of different pathogens. Recent studies have implicated lipid rafts in the cell uptake of *Mycobacterium bovis* (14), the malaria parasite *Plasmodium falciparum* (47), and some viruses, including simian virus 40 (39, 40) and murine leukemia virus (29).

The role of lipid rafts in HIV-1 entry is mostly unknown. Although direct evidence of the involvement of rafts in HIV-1 entry needs to be demonstrated, recent studies showing that the raft-resident glycosphingolipids Gb3 and GM3 promote the entry of a broad range of HIV-1 isolates (19) and the role of membrane cholesterol in HIV-1 entry (28) strongly suggest this possibility. In agreement with these observations, we report here that productive entry of X4 and R5 HIV-1 into $CD4^+$ T cells requires the presence of intact lipid rafts, most likely due to significant concentration of CD4 and colocalization of the HIV-1 receptors in these microdomains.

MATERIALS AND METHODS

Reagents. Recombinant gp120 from the X4 HIV-1 IIIB and mouse and rabbit anti-gp120 antibodies were purchased from Bartels Diagnostics. Paraformaldehyde, enzyme-linked immunosorbent assay (ELISA)-grade bovine serum albumin (BSA), *methyl*-β-cyclodextrin (MβCD), water-soluble cholesterol, biotin and peroxidase conjugates of cholera toxin subunit B (CT-B), and streptavidin-fluorescein isothiocyanate (FITC) were from Sigma. Alexa Fluor 488 and 594 conjugates of CT-B and streptavidin, Alexa Fluor 488- and 594-labeled goat anti-mouse and goat anti-rabbit IgG F(ab′) fragments, the Alexa Fluor 488 signal amplification kit for mouse antibodies, and the ProLong antifade kit were from Molecular Probes. Phycoerythrin (PE)-conjugated CD4, CXCR4, and CCR5 monoclonal antibodies and FITC-conjugated anti-CD71 and anti-CCR5 (2D7) antibodies were from BD Pharmingen. Rabbit polyclonal anti-CD71, mouse monoclonal anti-CD48, rabbit anti-CD4 (H-370), and goat anti-CCR5 (C-20) were from Santa Cruz Biotechnology and were used for Western blotting. Monoclonal CD4-FITC (13B8.2) was from Immunotech. Monoclonal anti-CXCR4 (clone 44716.111) and anti-CXCR4-FITC (clone 12G5) were from R&D Systems. Monoclonal anti-CXCR4, clone 4G10, was provided by C. Broder (Uniformed Services University of the Health Sciences, Bethesda, Md.).

Cell cultures. Jurkat T cells (clone E6-1 [ATCC TIB-152]), PM1 T cells, and CEMx174 cells were maintained in RPMI 1640 medium with L-glutamine (Invitrogen) supplemented with 10% fetal calf serum (FCS; Gemini Bio-Products, Calabasas, Calif.) and gentamicin (50 μg/ml).

Virus preparation and purification. Virus stock was prepared by transfecting 293T cells with NL4-3 or Ad8 (41) plasmid DNA. The culture supernatant containing virus was collected on day 3 after transfection and clarified by filtering it through a 0.45-μm-pore-size filter. The virus was concentrated and purified by ultracentrifugation through a cushion of 20% sucrose in phosphate-buffered saline (PBS). The pelleted virus was resuspended in PBS with 0.1% BSA, aliquoted, and stored frozen at −80°C. The virus titer was determined by the reverse transcriptase (RT) activity assay (43). For PCR analysis of HIV-1 entry, virus preparations were treated with RNase-free DNase (200 U/ml) for 1 h at room temperature to eliminate potential contamination with viral DNA.

Semiquantitative PCR analysis of HIV-1 entry. The cells were resuspended in RPMI–0.1% BSA (10^6 cells/ml) and immediately exposed to DNase-treated and sucrose gradient-purified HIV-1 NL4-3 or Ad8 (5 cpm of RT/cell) as described previously (43). After incubation with the virus, the cells were extensively washed to remove unbound virus and lysed in PCR lysis buffer consisting of 50 mM KCl, 10 mM Tris-HCl (pH 8.3), 2.5 mM $MgCl_2$, 0.1 mg of gelatin/ml, 0.45% Nonidet P-40, 0.45% Tween 20, and 100 μg of proteinase K/ml. After protein digestion for 2 h at 56°C and inactivation for 10 min at 95°C, serial dilutions of cell lysates were subjected to 25 to 30 cycles of PCR with *Taq* polymerase in a total volume of 50 μl containing 0.2 μM oligonucleotide primers in PCR SuperMix (Life Technologies). The PCR conditions and HIV-1-specific oligonucleotide primers detecting early R/U5 DNA were described previously (51). Amplification of the β-globin gene in cell lysates was used to control the amount of DNA in each sample. PCR products were analyzed by electrophoresis in 2% agarose gels and visualized by ethidium bromide staining.

Single-cycle infectivity assay. Plasmid DNA (15 μg) encoding envelope from the T-tropic HIV-1 clone HXB2 or vesicular stomatitis virus envelope (VSV-G) was cotransfected with pNL4-3Env(−)LUC(+) (5 μg) (8) into 293T cells using SuperFect (Qiagen). Forty-eight hours after transfection, the culture supernatants were collected, filtered through 0.45-μm-pore-size filters, and concentrated by ultracentrifugation through a cushion of 20% sucrose in PBS. CEMx174 cells (untreated or treated with 10 mM MβCD) were incubated for 1 h with standardized amounts of pseudotyped viruses (5 cpm of RT/cell) and washed, and the cultures were propagated for 48 h. After incubation, the cells were washed and lysed in 100 μl of lysis buffer (Promega). Luciferase activity was determined after adding 100 μl of Luciferase Assay Reagent (Promega) to 10 μl of cell lysate and counting the resultant scintillation for 10 s using a Monolight 2010 luminometer (Analytical Luminescence Laboratory). Background luciferase activities, determined by infection of cells with NL4-3 Env^- LUC^+ virions produced in the absence of envelopes, were negligible (180 relative light units for 10 s of counting).

[^{3}H]cholesterol labeling of cells. Labeling with [^{3}H]cholesterol was performed as described previously (17). PM1 T cells (2×10^7) were washed in serum-free RPMI 1640 medium and incubated for 3 h at 37°C in 20 ml of serum-free RPMI 1640 supplemented with 100 μCi of [1α,2α (n)-^{3}H]cholesterol (Amersham Pharmacia Biotech). The cells were then washed in RPMI 1640 medium with 10% FCS and incubated for 20 h at 37°C in RPMI 1640 with 10% FCS to equilibrate the radiolabeled cholesterol with the cellular cholesterol pool (17). Subsequently, cholesterol from one part of the radiolabeled cells was extracted with MβCD as described below. Finally, Triton X-100 lysates prepared from untreated and cholesterol-depleted cells were ultracentrifuged in a sucrose density gradient and fractionated (see "Biochemical isolation of lipid rafts" below). ^{3}H radioactivity in gradient fractions was analyzed using a Beckman liquid scintillation counter.

Cholesterol depletion. Before extraction of cholesterol, the cells were washed twice with RPMI. The cells (2×10^7) were incubated with 10 mM MβCD in RPMI supplemented with 0.1% BSA (ELISA grade; Sigma) for 30 min at 37°C on a rocking platform. Under these conditions, cell viability was not significantly affected, as determined by trypan blue exclusion. As controls, the cells were either exposed to medium alone or were treated with MβCD and subsequently reconstituted with water-soluble cholesterol (400 μg/ml) for 1 h at 37°C. After incubation, the cells were washed twice with ice-cold RPMI–0.1% BSA before being used.

Biochemical isolation of lipid rafts. Cells (2×10^7 to 5×10^7) were washed twice with ice-cold PBS and lysed on ice for 30 min in 1 ml of 1% Triton X-100 TNE lysis buffer (25 mM Tris [pH 7.5], 150 mM NaCl, 5 mM EDTA) supplemented with protease inhibitor cocktail (Complete; Roche Molecular Biochemicals). The cell lysates were homogenized with 10 strokes of a Dounce homogenizer and centrifuged for 5 min at $720 \times g$ at 4°C in a microcentrifuge to remove insoluble material and nuclei. The supernatant was mixed with 1 ml of 80% sucrose in lysis buffer, placed at the bottoms of ultracentrifuge tubes, and overlaid with 6 ml of 30% and 3 ml of 5% sucrose in TNE lysis buffer. The lysates were ultracentrifuged at 4°C in a SW41 rotor (Beckman) for 16 to 18 h at 38,000 rpm. After centrifugation, the Triton X-100-insoluble, low-density material containing rafts was visible as a band migrating on the boundary between 5 and 30% sucrose. Eleven 1-ml fractions were collected from the top with Auto Densi-Flow (Labconco) and analyzed immediately by Western blotting or stored at −80°C.

Western blot analysis. Aliquots of 40 μl of individual sucrose gradient fractions were analyzed by sodium dodecyl sulfate-polyacrylamide gel electrophoresis (SDS-PAGE) on 10% polyacrylamide gels. The proteins were transferred to supported nitrocellulose membranes and probed with specific antibodies as described previously (41). Bound antibodies were detected with the SuperSignal

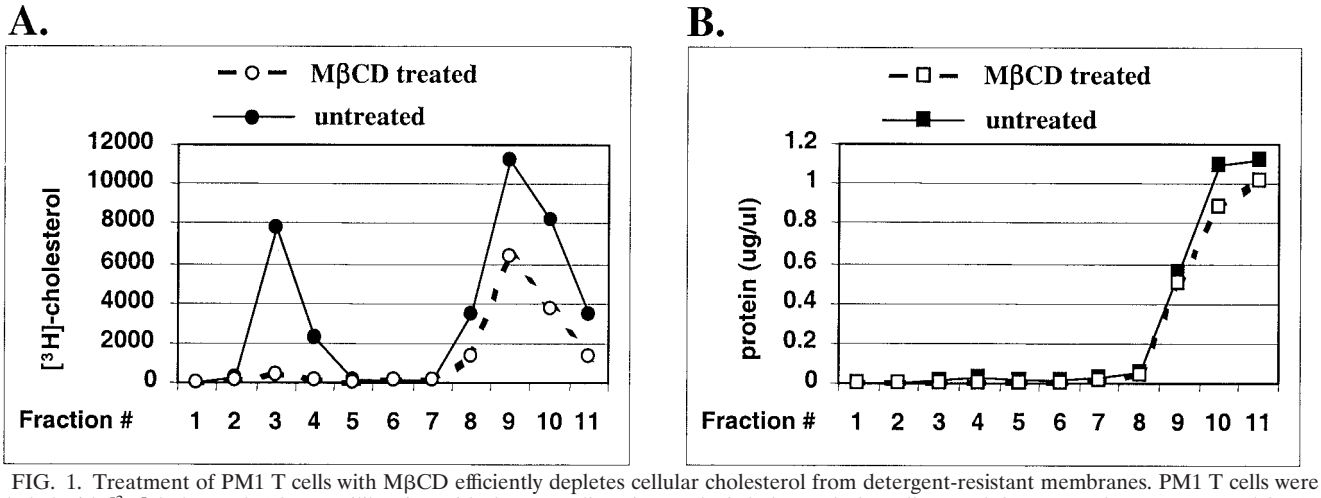

FIG. 1. Treatment of PM1 T cells with MβCD efficiently depletes cellular cholesterol from detergent-resistant membranes. PM1 T cells were labeled with [^{3}H]cholesterol. After equilibration with the nonradioactive pool of cholesterol, the cells were left untreated or were treated for 30 min at 37°C with 10 mM MβCD, homogenized in 1% Triton X-100 TNE buffer, and ultracentrifuged in a sucrose density gradient as detailed in Materials and Methods. One-milliliter fractions were collected from the top of the gradient. Detergent-insoluble material (lipid rafts) is present in fractions 3 and 4. The ^{3}H radioactivity (A) and protein content (B) in each gradient fraction from untreated and MβCD-treated cells are shown.

West Dura substrate (Pierce). The protein concentration was determined with the bicinchoninic acid protein assay reagent (Pierce).

Flow cytometry. Expression of CD4 and CXCR4 on the surfaces of PM1 T cells was evaluated by flow cytometry as described previously (43). The cells, preincubated on ice for 30 min in PBS–1% BSA, were subsequently collected by centrifugation and incubated for 30 min on ice with FITC-conjugated monoclonal antibodies against CD4 (13B8.2) or CXCR4 (12G5), washed twice with PBS–1% BSA and once with PBS, and fixed in 4% formaldehyde in PBS for 30 min on ice. Samples were analyzed on a Becton Dickinson FACScan within 2 h of immunofluorescence staining.

Raft aggregation and confocal microscopy. A total of 10^6 PM1 T cells expressing CD4 as well as CXCR4 and CCR5 receptors (42) were washed in serum-free RPMI and incubated on ice for 20 min with PBS supplemented with 0.1% BSA (ELISA grade). The cells were incubated on ice for 30 min with fluorescently labeled monoclonal antibodies at concentrations suggested by the manufacturer followed by extensive washing with ice-cold PBS–0.2% BSA. To investigate the presence of HIV-1 receptors in lipid rafts, the cells were first incubated for 30 min on ice with biotinylated CT-B and washed extensively with PBS–0.2% BSA. Lipid raft aggregation was initiated by incubation with streptavidin-conjugated FITC in the presence of PE-conjugated CD4, CXCR4, or CCR5 monoclonal antibodies for 30 min at 37°C. After being washed twice with ice-cold PBS-BSA, the cells were fixed on ice for 30 min with fresh 4% paraformaldehyde. To analyze colocalization of CD4 receptor with CXCR4 and CCR5, PM1 T cells were first incubated with anti-CD4 (clone 13B8.2) or with anti-CXCR4 (clone 44716.111) antibody and washed, and aggregation was initiated by the incubation of the cells for 20 min at 37°C with dialyzed Alexa Fluor 594-conjugated goat anti-mouse IgG F(ab′) antibody fragments. After being washed with ice-cold PBS-BSA, the cell aliquots were incubated on ice for 30 min with anti-CCR5-FITC (clone 2D7), anti-CXCR4-FITC (clone 12G5), or anti-CD4-FITC (clone 13B8.2). In addition, lipid raft ganglioside GM1 was identified by incubation with Alexa Fluor 488-conjugated CT-B (10 μg/ml). The cells were washed, fixed, and mounted using a ProLong antifade kit. Fluorescently labeled cells were analyzed with a Nikon PCM 2000 laser scanning confocal microscope with 60× objective lenses. The images were processed using Photoshop software (Adobe).

RESULTS

Cholesterol extraction disintegrates lipid rafts in CD4$^+$ T cells. The effectiveness of cholesterol extraction and raft disintegration was examined by analysis of the distribution of cholesterol and raft-specific components in cell membrane microdomains before and after extraction of cholesterol with MβCD (23, 55). Since rafts resist solubilization by cold nonionic detergents and float to low density during sucrose gradient centrifugation, proteins and lipids detected in low-density fractions are considered to be associated with rafts (52).

Distribution of cholesterol was analyzed in gradient fractions prepared from cells equilibrated with radiolabeled cholesterol (see Materials and Methods). Analysis of the [^{3}H]cholesterol content in gradient fractions showed that in fractions 3 and 4 the levels of radiolabeled cholesterol were reduced by 95% following MβCD treatment (Fig. 1A). In contrast, cholesterol levels in soluble fractions 9 and 10 were reduced by 44%, suggesting that cholesterol present in these fractions may also contain an intracellular pool of cholesterol not accessible for extraction. Analysis of the protein contents of gradient fractions indicates that fractions 3 and 4 contain significantly lower levels of proteins than fractions 9 to 11 (Fig. 1B), i.e., the concentration of proteins in fraction 3 was 0.015 μg/μl in comparison with 1.09 μg/μl in fraction 10. Thus, the cholesterol/protein ratio is significantly higher in detergent-resistant fractions than in detergent-soluble fractions. These properties strongly suggest that lipid rafts are present in gradient fractions 3 and 4. This conclusion was further confirmed by the analysis of the distribution of markers specific for rafts and nonraft membranes. In untreated Jurkat CD4$^+$ T cells, the raft markers ganglioside GM1 and glycosylphosphatidylinositol (GPI)-anchored CD48 were predominantly localized in fractions 3 and 4 (Fig. 2A). In contrast, a nonraft marker, transferrin receptor CD71 (22), was confined to detergent-soluble fractions (Fig. 2B). Extraction of cholesterol had different effects on these raft and nonraft markers. Expression and localization of CD71 in PM1 T-cell membranes remained unchanged after cholesterol extraction (Fig. 2B). In contrast, cholesterol was required to maintain the association of GM1 and CD48 with lipid rafts (Fig. 2A). Altogether, extraction of cholesterol from cell membranes by MβCD efficiently destabilized lipid raft integrity.

Depletion of cholesterol inhibits HIV-1 entry into CD4$^+$ T cells independently of virus tropism. To investigate whether intact lipid rafts are required for the entry of HIV-1 into CD4$^+$

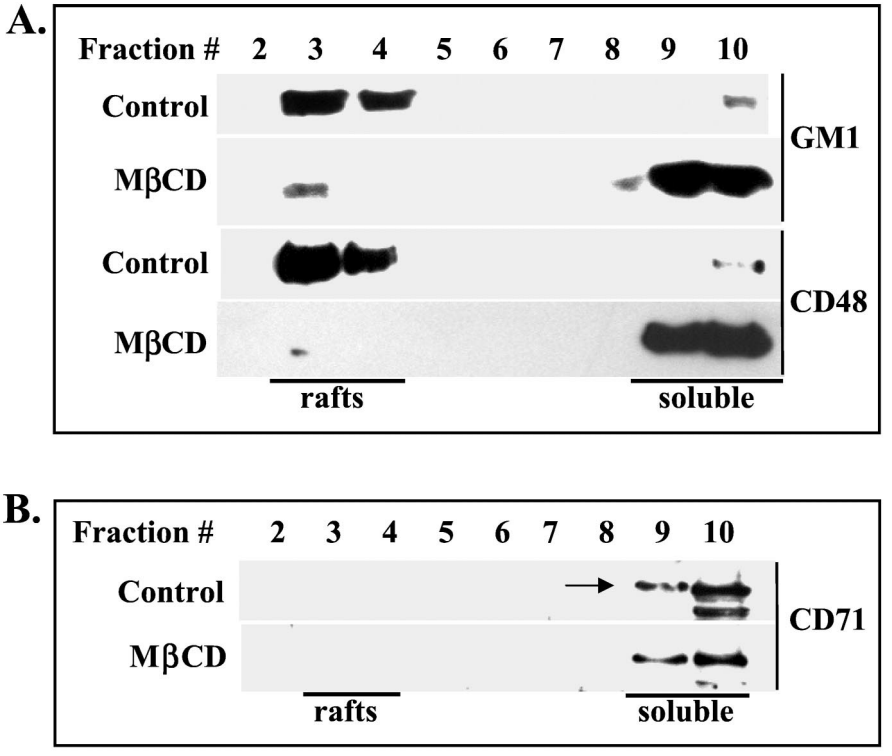

FIG. 2. Cholesterol depletion disintegrates lipid rafts in PM1 T cells. The cells were left untreated (control) or were treated with 10 mM MβCD to extract cholesterol. Triton X-100 cell lysates were fractionated on a sucrose density gradient as described in Materials and Methods. (A) Equal volumes (40 μl) of individual fractions were resolved by SDS-PAGE, transferred to a nitrocellulose membrane, and probed with peroxidase-conjugated CT-B to detect raft-resident ganglioside GM1 or with mouse monoclonal anti-CD48 antibody to detect raft-specific GPI-linked CD48 antigen. (B) The nonraft membrane transferrin receptor CD71 (arrow) was detected in gradient fractions using rabbit anti-CD71 antibodies.

T lymphocytes, cholesterol from the plasma membrane was extracted with MβCD and virus entry was monitored by a semiquantitative PCR using primers that detect the accumulation of the early products (R/U5) of reverse transcription (43, 51). To avoid the possibility that newly synthesized cholesterol and/or cholesterol from internal compartments restores rafts and affects HIV-1 entry, incubation of MβCD-treated cells with the virus was continued for only 1 h at 37°C.

Entry of HIV-1 NL4-3 into MβCD-treated Jurkat T cells was reduced about 10-fold in comparison with virus entry into untreated cells (Fig. 3A; NL4-3). The inhibition of HIV-1 entry was not due to the potential toxicity of MβCD, since cells exposed to cyclodextrin and subsequently replenished with exogenous cholesterol (Fig. 3A; MβCD/cholesterol) supported virus entry to the levels observed in untreated cells. As a negative control for HIV-1 entry, the cells were incubated with NL4-3 for 1 h at 4°C to allow virus binding without internalization. Very low levels of R/U5 signals could be detected in cells exposed to virus at 4°C (Fig. 3A). This may suggest the presence of low levels of intravirion early RT products inaccessible to DNase treatment during preparation of virus stock. The monoclonal anti-CD4 antibody (Q4120) or an antagonist of CXCR4 receptor (AMD3100) efficiently blocked entry of the virus into Jurkat T cells (Fig. 3B).

Inhibition of HIV-1 entry after cholesterol extraction was not restricted to $CD4^+$ Jurkat T cells and was also observed in CCR5-positive PM1 T cells. As shown in Fig. 3C, the entry of X4 NL4-3 into cholesterol-depleted PM1 cells was reduced about eightfold; however, it was restored to the levels observed in untreated cells after incubation with exogenous cholesterol for 1 h at 37°C.

Inhibition of HIV-1 entry after cholesterol extraction was independent of virus tropism. As shown in Fig. 3D, entry of R5 Ad8 HIV-1 was significantly inhibited in MβCD-treated cells. However, virus entry was restored by readdition of exogenous cholesterol. In conclusion, these results strongly support the notion that cholesterol is required for efficient entry of both X4 and R5 HIV-1, probably by maintaining lipid raft integrity.

Cholesterol depletion inhibits receptor-mediated, productive HIV-1 infection. HIV-1 may enter the cells by both receptor-mediated membrane fusion and endocytosis (11, 34, 48). It is believed that HIV-1 entry through an endocytic pathway does not contribute to productive infection. Thus, to investigate how the depletion of cholesterol may affect these entry pathways, we employed a single-cycle infection assay. In this assay, HIV-1 virions were produced by cotransfection of envelope expression vectors with a reporter construct, pNL4-3Env(−)LUC(+) (7). Virions pseudotyped with T-tropic HIV-1 clone HXB2 envelope or with the envelope glycoprotein G from VSV (VSV-G) were used to infect CEMx174 cells. In contrast to HIV-1 envelope, VSV-G envelope targets virions for entry via endocytosis and fusion with acidified endosomes, allowing subsequent viral replication steps to occur (1). The amount of luciferase activity measured in cells infected with pseudotyped viruses serves as an indirect estimation of viral entry, integration, and transcriptional activity in

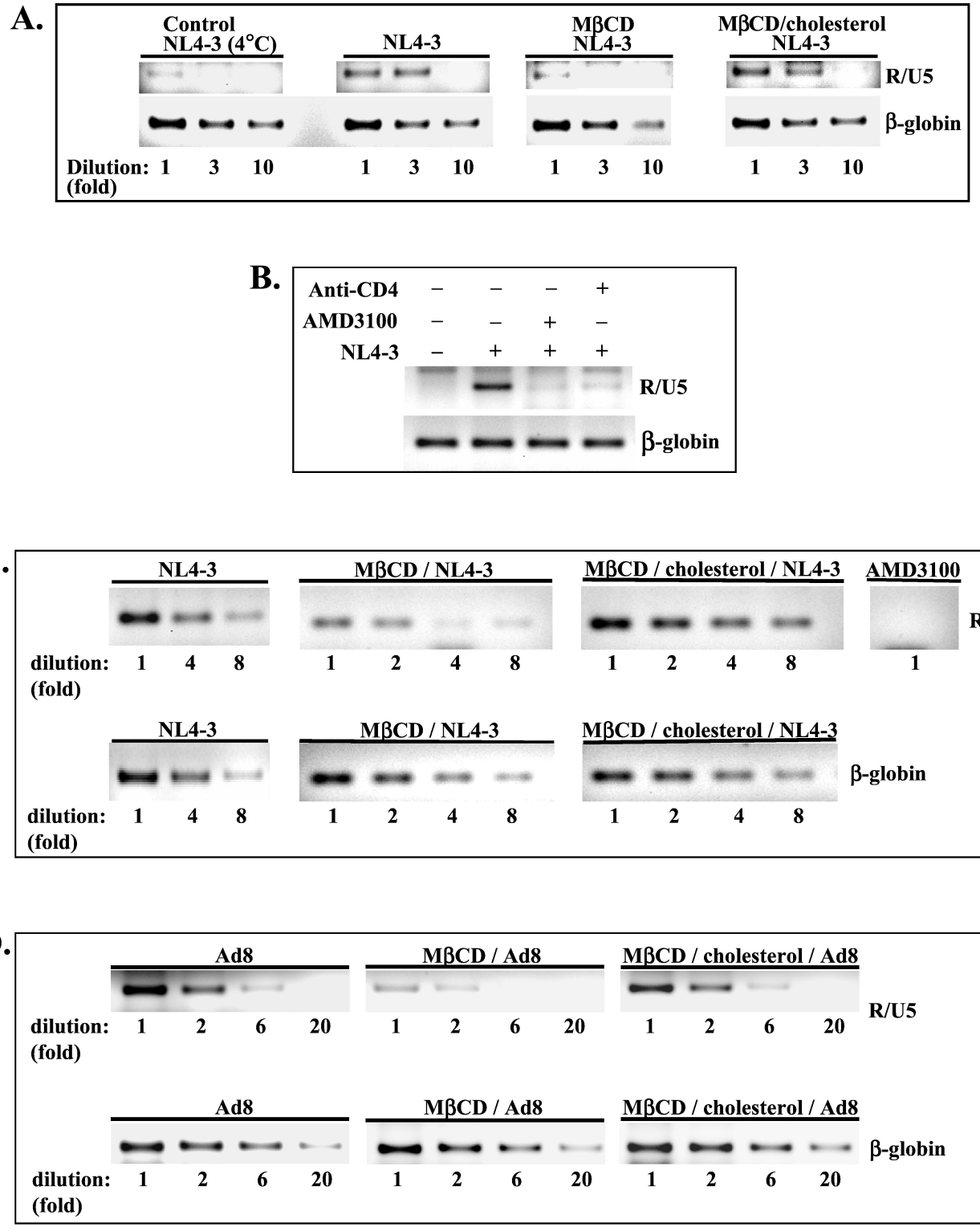

FIG. 3. Depletion of cholesterol inhibits HIV-1 entry into $CD4^+$ T cells independently of virus tropism. HIV-1 entry into Jurkat T cells (A and B) and PM1 T cells (C and D) was analyzed by semiquantitative PCR. Cells untreated, MβCD treated, or MβCD treated and reconstituted with cholesterol for 1 h at 37°C (MβCD/cholesterol) were infected (5 cpm of RT/cell) with X4 NL4-3 (A and C) or R5 Ad8 HIV-1 (D). One hour after infection, the cells were lysed, and PCR amplification of serially diluted cell lysates was performed with R/U5 primers specific for strong-stop DNA as described in Materials and Methods. Amplification of the β-globin gene was used to control the amount of DNA in each sample. PCR products were resolved by electrophoresis in 2% agarose gels and stained with ethidium bromide. (B) Inhibition of HIV-1 entry into Jurkat cells pretreated with monoclonal anti-CD4 antibody Q4120 (10 μg/ml) or with an antagonist of CXCR4 receptor, AMD3100 (1 μg/ml). (C) AMD3100 also inhibits HIV-1 NL4-3 entry into PM1 T cells.

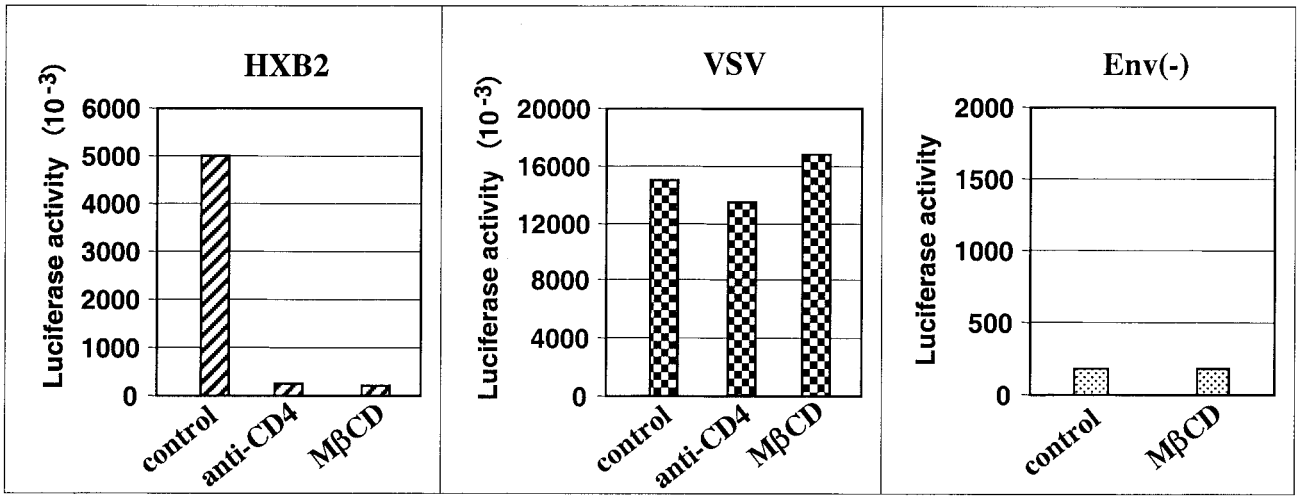

FIG. 4. Cholesterol depletion inhibits productive infection by receptor-mediated membrane fusion but not endocytosis. CEMx174 cells, untreated (control) or treated for 30 min with 10 mM MβCD, were infected for 1 h with envelope-defective NL4-3 Env$^-$ LUC$^+$ virions alone, [Env(−)] or with virions pseudotyped with HXB2 or VSV envelope (5 cpm of RT/cell). After extensive washing, the cells were cultivated and collected 48 h later. Luciferase activity in 10 μl of cell lysates (expressed as relative light units) was determined using luciferase assay reagent as described in Materials and Methods. As a control, the cells were pretreated with anti-CD4 Q4120 (10 μg/ml) for 30 min before infection with viruses. The results are representative of two independent experiments.

control and MβCD-treated cells. The results of a representative experiment are shown in Fig. 4. Negligible levels of luciferase activity could be detected in lysates prepared from cells infected with virions generated by transfection of the reporter vector alone [Fig. 4; Env(−)]. As a control, the cells were preincubated with anti-CD4 antibody Q4120 before infection with pseudotyped viruses. As expected, productive entry of HXB2-pseudotyped virus was inhibited by 96% after preincubation of the cells with anti-CD4 antibody. In contrast, productive entry of virus pseudotyped with VSV-G envelope was not affected by blocking the CD4 receptor with anti-CD4 antibody. Extraction of cholesterol resulted in 95% inhibition of luciferase activity in cells infected with virus pseudotyped with HXB2 envelope but did not affect expression of luciferase activity in cells infected with virus pseudotyped with VSV-G envelope. These results demonstrate that extraction of cholesterol and subsequent disruption of lipid rafts dramatically inhibits productive infectivity of viruses pseudotyped with HIV-1 envelope but does not affect entry of viruses through an endocytic, raft-independent pathway.

Extraction of cholesterol with MβCD does not significantly change the surface expression of CD4 or CXCR4. We next investigated whether the reduced HIV-1 entry into cholesterol-depleted cells results from the downregulation of virus receptors in MβCD-treated cells. The cell surface expression of CD4 and CXCR4 in PM1 T cells was analyzed by flow cytometry. No change in the cell surface expression of CD4 receptor was observed after depletion of cholesterol (Fig. 5). However, the expression of CXCR4 was moderately changed in MβCD-treated cells. Although the reason for the bimodal CXCR4 expression pattern is unclear, we speculate that it may result from conformational changes in a subpopulation of CXCR4 receptors after extraction of cholesterol that affected the epitope recognized by anti-CXCR4 antibody. In conclusion,

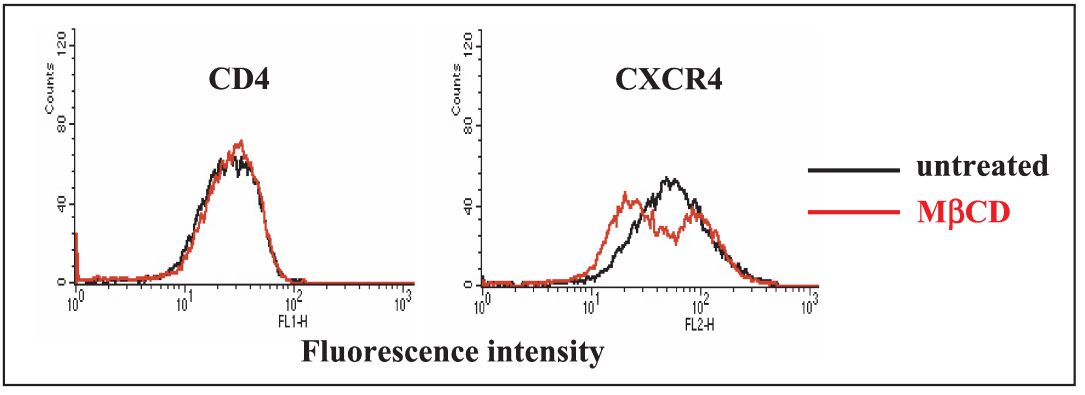

FIG. 5. Cholesterol depletion does not significantly affect the surface expression of CD4 and CXCR4 receptors. Untreated PM1 T cells or cells treated with 10 mM MβCD were stained for 30 min on ice with FITC-conjugated monoclonal antibodies against CD4 (13B8.2) or CXCR4 (12G5) and subsequently analyzed by flow cytometry as described in Materials and Methods.

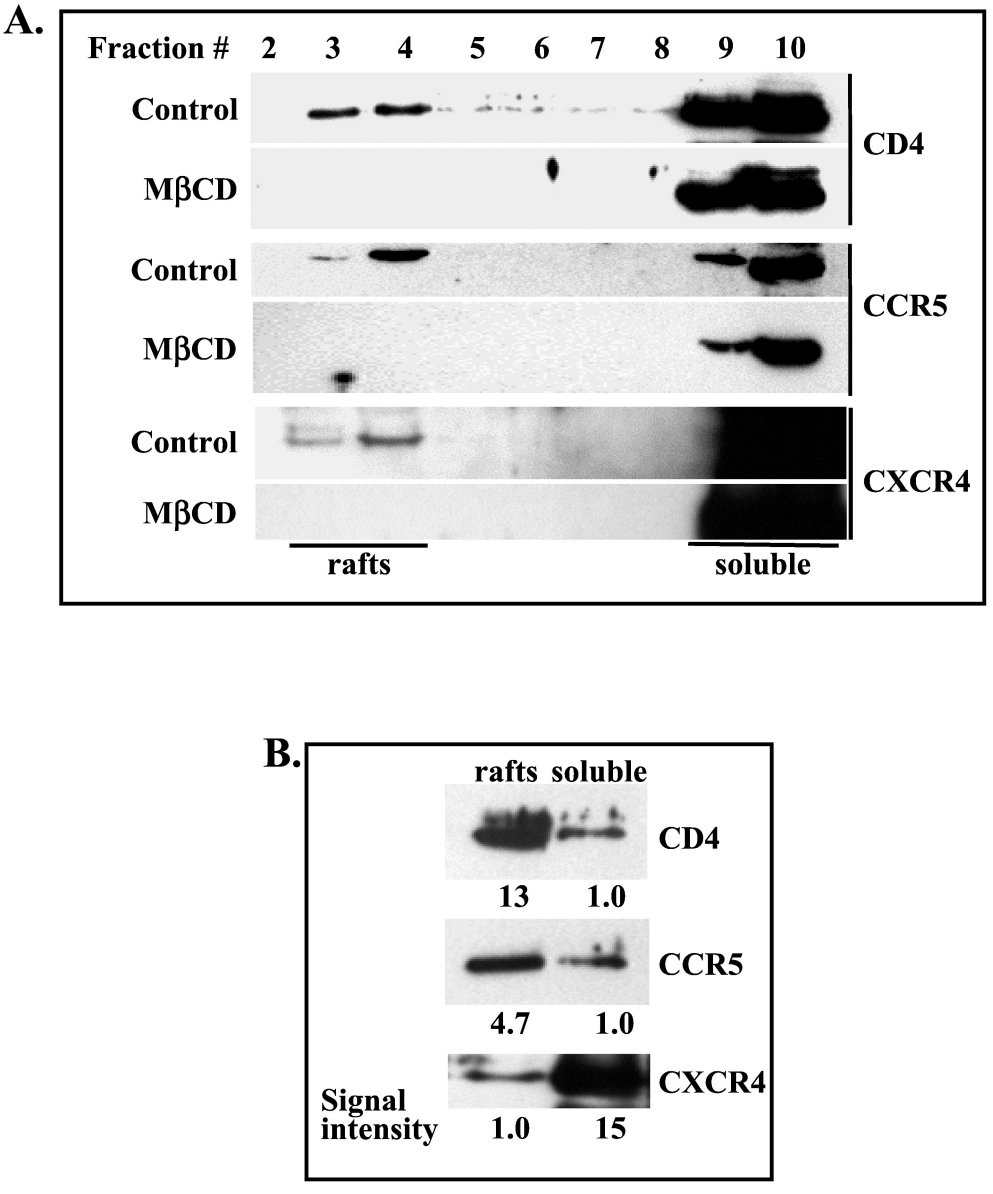

FIG. 6. CD4, CCR5, and CXCR4 associate to different extents with detergent-resistant lipid raft fractions. Untreated (control) or MβCD-treated PM1 T cells were lysed with Triton X-100 lysis buffer, and cell postnuclear extracts were fractionated on a sucrose density gradient as described in Materials and Methods. (A) Equal volumes (40 μl) of individual fractions were resolved by SDS-PAGE, transferred to a nitrocellulose membrane, and probed with anti-CD4 (H-370), anti-CCR5 (C-20), or anti-CXCR4 (4G10) antibodies. (B) Equal amounts of protein (1 μg) from combined raft fractions 3 and 4 or soluble fractions 9 and 10 were resolved on SDS-PAGE and analyzed by Western blotting as described above. The intensities of specific bands representing CD4, CCR5, and CXCR4 receptors were calculated by densitometry.

our observation suggests that cholesterol is an important cofactor in HIV-1 entry possibly because it preserves raft integrity and therefore allows the accumulation of HIV-1 receptors in lipid rafts.

CD4, CCR5, and CXCR4 associate to different extents with membrane rafts. Biochemical analysis. To examine whether HIV-1 receptors associate with raft microdomains, detergent-insoluble membrane rafts were isolated from postnuclear supernatants prepared from PM1 T cells lysed with ice-cold Triton X-100 and ultracentrifuged on sucrose gradient (57). Aliquots of gradient fractions were resolved on SDS-PAGE, and the expression of HIV-1 receptors was analyzed by Western blotting. Figure 6A shows that CD4, CCR5, and CXCR4 colocalize with detergent-insoluble rafts (fractions 3 and 4). These results were further supported by the observation that expression of the receptors in lipid rafts, but not in nonraft fractions, was abolished by extraction of cholesterol with MβCD (Fig. 6A).

HIV-1 receptors can also be detected in detergent-soluble fractions (fractions 9 and 10). To quantitate the expression of CD4, CCR5, and CXCR4 in raft and soluble fractions, raft fractions 3 and 4 and soluble fractions 9 and 10 were combined and an equal amount of protein from each pool was resolved on SDS-PAGE and analyzed by Western blotting (Fig. 6B).

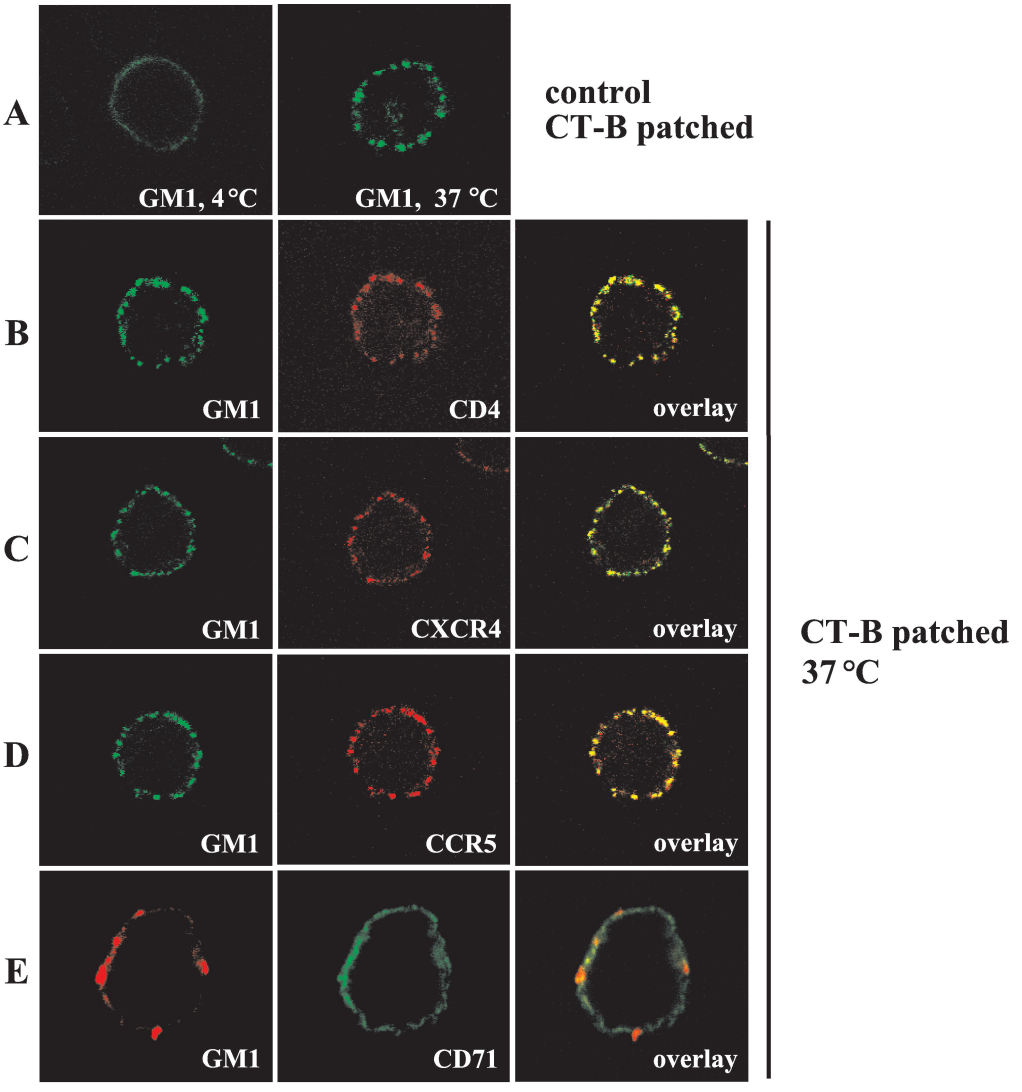

FIG. 7. HIV-1 receptors localize to lipid rafts. PM1 T cells were incubated on ice with biotinylated CT-B, which specifically binds to the raft-resident ganglioside GM1. Subsequently, the cells were incubated on ice with streptavidin conjugated with FITC (A to D) or Alexa Fluor 594 (E). Raft aggregation was initiated by incubation of the labeled cells at 37°C for 30 min in the absence (A) or in the presence of PE-conjugated CD4, CXCR4, or CCR5 monoclonal antibody (B to D) or FITC-conjugated CD71 monoclonal antibody (E) as described in Materials and Methods. CT-B-patched cells were fixed and visualized by confocal microscopy. Single confocal sections are shown. The colocalization of HIV-1 receptors with the raft marker GM1 is presented (overlay). (A) Control cells incubated with biotinylated CT-B and streptavidin-FITC at 4°C show uniform distribution of GM1 before raft aggregation.

The results show that CD4 and CCR5 were significantly enriched in lipid rafts (13- and 4.7-fold, respectively). However, the majority of CXCR4 (approximately 93%) was detected in non-raft-soluble fractions. The reason for the differential association of CXCR4 and CCR5 with lipid rafts is presently unknown but may be related to the constitutive association of CCR5 but not CXCR4 with CD4 (56).

Analysis of HIV-1 receptor localization in lipid rafts by confocal microscopy. To confirm the biochemical results obtained in flotation gradients, the association of HIV-1 entry receptors with lipid rafts was investigated in intact cells by confocal microscopy using fluorescently labeled CT-B, which specifically binds to a raft-resident ganglioside GM1 (22).

To examine the presence of HIV-1 receptors in rafts, we analyzed whether ligation of GM1 with CT-B subunit and the consequent aggregation of rafts affects the localization of HIV-1 receptors. PM1 T cells, which express CD4 as well as CXCR4 and CCR5, were first exposed for 30 min on ice to biotinylated CT-B and extensively washed, and raft aggregation was initiated by a 30-min incubation at 37°C with fluorescently labeled streptavidin in the presence of PE-conjugated monoclonal antibodies against CD4, CXCR4, or CCR5 or FITC-conjugated anti-CD71 antibodies.

Treatment of PM1 T cells with CT-B–biotin/streptavidin–FITC complex alone at 4°C resulted in a uniform pattern of plasma membrane staining; however, 30-min incubation at 37°C led to formation of large GM1 patches (Fig. 7A). Incubation of the cells simultaneously with CT-B–biotin/streptavi-

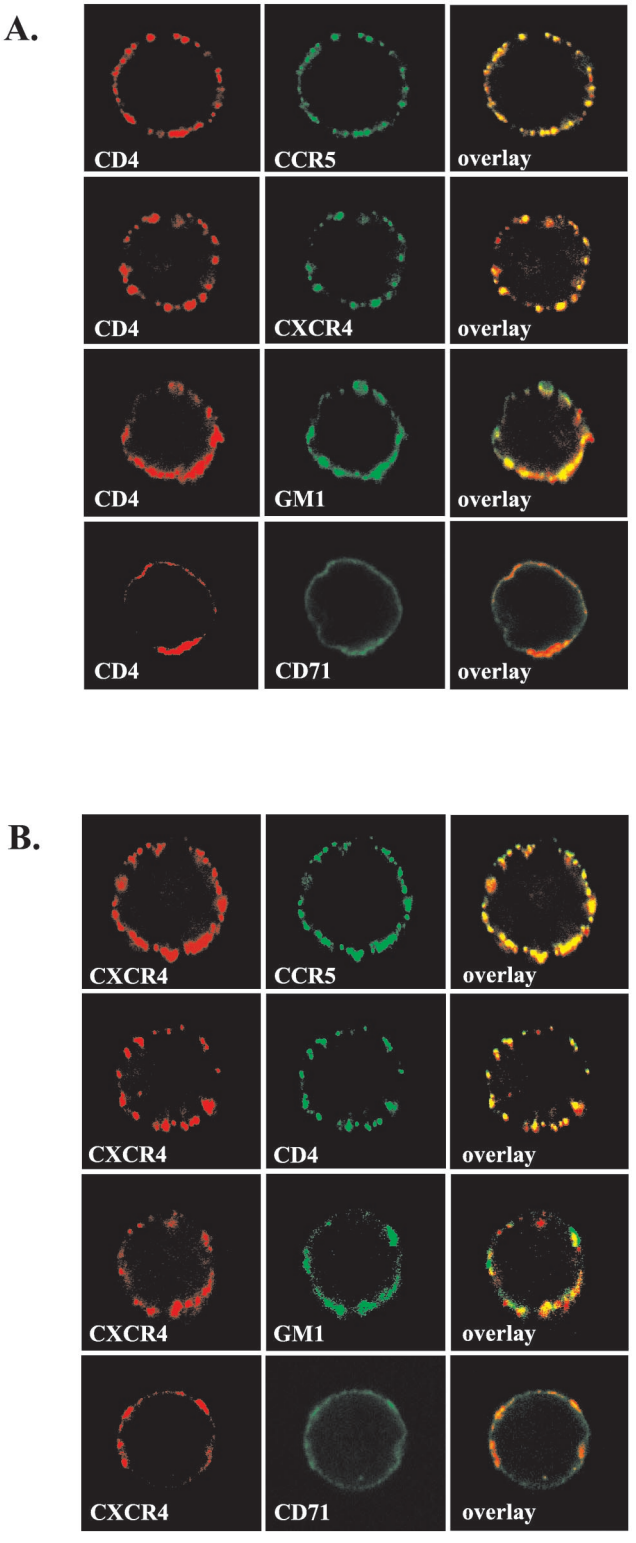

FIG. 8. CD4 receptors colocalize with CCR5 and CXCR4 coreceptors. PM1 T cells were incubated with anti-CD4 (A) or anti-CXCR4 (B) monoclonal antibody, and the receptor aggregation was induced by incubating the cells at 37°C for 20 min with Alexa Fluor 594-conjugated goat anti-mouse IgG F(ab′) antibody fragments. Following the aggregation of CD4 or CXCR4 receptors, the cells were labeled with FITC-conjugated antibodies against CCR5 and CXCR4 (A) or against CCR5 and CD4 (B) as described in Materials and Methods. Lipid raft ganglioside GM1 was identified by incubation with Alexa Fluor 488-conjugated CT-B, and the nonraft marker CD71 was visualized using FITC-conjugated anti-CD71 antibody. Fluorescently labeled cells were analyzed by confocal microscopy as described in the legend to Fig. 7.

din–FITC and PE-conjugated antibodies specific for CD4, CXCR4, or CCR5 (Fig. 7B to D) resulted in substantial colocalization of these receptors with GM1 patches. In contrast, GM1 did not colocalize significantly with the nonraft marker CD71 (Fig. 7E). The observed sequestration of HIV-1 receptors by lateral cross-linking of GM1 suggests that virus receptors and GM1 reside in the same lipid environment in the plasma membrane and indicates that HIV-1 receptors are associated constitutively, yet not exclusively, with lipid rafts.

CD4 receptor colocalizes with CCR5 and CXCR4 in cell membranes of PM1 T cells. To investigate whether the HIV-1 receptors localize in the same or different membrane microdomains, we analyzed whether the aggregation of a particular receptor affects the distribution of other receptors. PM1 T cells were first incubated with monoclonal anti-CD4 or anti-CXCR4 antibody, and the receptor aggregation was stimulated by incubating the cells at 37°C for 20 min with Alexa Fluor 594-conjugated goat anti-mouse IgG F(ab′) antibody fragments. Following the aggregation of CD4 receptors, the cells were incubated on ice with FITC-conjugated anti-CCR5 or anti-CXCR4 antibodies. Similarly, following CXCR4 receptor aggregation, the cells were incubated with anti-CD4-FITC or anti-CCR5-FITC. Lipid raft ganglioside GM1 was identified by incubation with Alexa Fluor 488-conjugated CT-B. The nonraft marker CD71 transferrin receptor was visualized with FITC-conjugated anti-CD71 antibodies. The cell surface distribution of the receptors was visualized by confocal microscopy. Figure 8A shows that CCR5 and CXCR4 receptors coaggregated with cross-linked CD4 receptor. Similarly, CCR5 and CD4 coaggregated with cross-linked CXCR4 (Fig. 8B). In contrast, CD4 and CXCR4 colocalized with CD71 (nonraft) to significantly lower levels, although some areas of colocalization can be found (Fig. 8). Since HIV-1 receptors colocalize with raft-resident ganglioside GM1 (Fig. 7 and 8), these results suggest that in PM1 T cells, a fraction of CD4 receptors may be localized in the same rafts as CCR5 and CXCR4 receptors. However, we cannot exclude the possibility that more than one type of raft exists on the cell surface, and these may include detergent-sensitive microdomains that contain a majority of CXCR4 with some CD4 or CCR5 receptors.

HIV-1 envelope gp120 associates with lipid rafts in Jurkat T cells. Since HIV-1 receptors are present in lipid rafts, we next investigated whether the HIV-1 gp120 envelope was able to interact with raft microdomains. Jurkat T cells were incubated with recombinant HIV-1 gp120 IIIB, and after a 30-min incubation on ice, the cells were extensively washed and exposed for 10 min at 37°C to rabbit anti-gp120 polyclonal antibody to induce cross-linking. After the incubation, postnuclear supernatants prepared from Triton X-100 cell lysates were ultracentrifuged in a sucrose density gradient. Aliquots of gradient fractions were resolved on SDS-PAGE, and the presence of gp120 was visualized by Western blotting using anti-gp120 antibody (Fig. 9A). The results show that gp120 could be detected in detergent-insoluble rafts (fractions 3 and 4) as well as

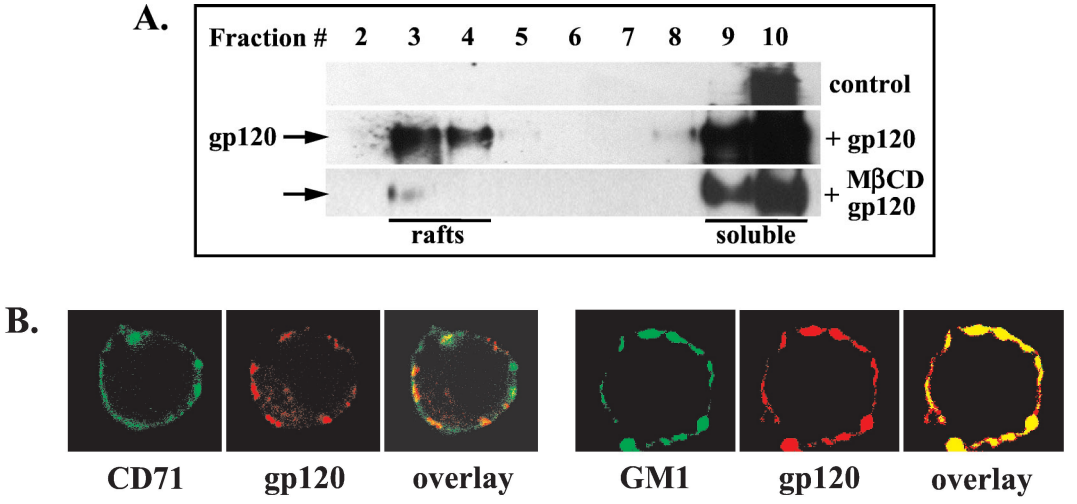

FIG. 9. HIV-1 envelope gp120 associates with lipid rafts. (A) Jurkat T cells, untreated or treated with 10 mM MβCD, were incubated for 30 min on ice with recombinant HIV-1 gp120 IIIB (10 μg/ml). The cells were washed to remove unbound gp120 and then were exposed for 10 min at 37°C to rabbit anti-gp120 antibody to induce cross-linking. The cells were lysed in Triton X-100 buffer, and the postnuclear extracts were fractionated in a sucrose density gradient. An aliquot of each fraction (40 μl) was resolved on SDS-PAGE, and gp120 was visualized by Western blotting as described in Materials and Methods. A signal present in fraction 10 of the control (cells not exposed to gp120) represents nonspecific binding of polyclonal antibody. (B) Membrane-bound HIV-1 gp120 colocalizes preferentially with lipid rafts. Distribution and colocalization of the nonraft marker CD71 (transferrin receptor) and the raft marker GM1 with gp120 were analyzed by confocal microscopy as described in Materials and Methods.

in soluble fractions. A signal present in fraction 10 of the control (cells not incubated with gp120) most likely represents nonspecific binding of polyclonal antibody.

The association of gp120 with lipid rafts was further confirmed by extracting cholesterol with MβCD and subsequent incubation of the cells with gp120. After the treatment, gp120 was predominantly associated with detergent-soluble fractions (Fig. 9A; gp120 plus MβCD). Binding of gp120 to lipid rafts was verified by confocal microscopy. Figure 9B shows that gp120 does not colocalize significantly with the transferrin receptor, CD71 (a nonraft marker), but does colocalize with GM1, a raft marker.

HIV-1 binding triggers raft aggregation and cocapping of HIV-1 receptors in PM1 cells. To investigate whether HIV-1 virions associate with lipid rafts in intact cells, we used confocal microscopy. PM1 T cells were incubated on ice for 30 min without virus or with purified HIV-1 NL4-3 (5 cpm of RT/cell) and then incubated at 37°C for 45 min. After the incubation, the cells were fixed with paraformaldehyde and the cell surface distribution of HIV-1 gp120 and CCR5 receptor was analyzed using fluorescently labeled monoclonal antibodies. GM1 was detected with Alexa Fluor 594-conjugated CT-B. Figure 10, top row, shows that in control cells incubated in the absence of HIV-1, GM1 and CCR5 receptors are rather evenly distributed over the cell surface. Incubation of the cells with HIV-1 dramatically changed the observed pattern of raft and receptor distribution. Rafts became polarized and formed well-developed caps that contained CCR5 receptors as well as HIV-1 envelope gp120 (Fig. 10, middle three rows). Furthermore, gp120 aggregates did not colocalize extensively with the nonraft CD71 receptor (Fig. 10, fourth row).

The presence of gp120 in rafts after incubation of the cells with virions most likely reflects interaction of the virus envelope with CD4 or CD4 and CXCR4 receptors. Interestingly, these results show that CCR5 receptors become aggregated in rafts despite the fact that CCR5 is not engaged by X4 NL4-3. In addition, coaggregation of CCR5 with virion gp120 could be disrupted by treatment with MβCD (Fig. 10, bottom row). There are at least two likely explanations for these observations. First, CCR5 may colocalize with CD4 receptors (Fig. 8A), and the engagement of CD4 by HIV-1 and raft aggregation will result in concomitant clustering of CCR5 receptors. Second, CCR5 receptors may be present in the same rafts as CXCR4 (Fig. 8B) and thus become clustered after HIV-1 binding to CXCR4 receptors and raft aggregation. These possibilities are not mutually exclusive and corroborate our observations that CD4 receptors colocalize with CCR5 and CXCR4 in PM1 cell membrane microdomains.

DISCUSSION

Accumulating data suggest that lipid rafts may be involved in the assembly and budding of HIV-1 (2, 18, 36, 38). However, the role of lipid rafts in HIV-1 entry is not well understood. Recent findings suggesting a role of cholesterol in HIV-1 entry (28) strongly support our hypothesis that cholesterol-rich lipid rafts represent binding and entry sites for productive HIV-1 infection. Thus, in this study, we have investigated the engagement of lipid rafts in the HIV-1 entry process and have shown that HIV-1 receptors likely colocalize in the same microdomains.

Insolubility in cold nonionic detergents is a key feature of lipid rafts. We have shown that Triton X-100 detergent-resistant fractions prepared from $CD4^+$ T cells have characteristics of lipid rafts. These fractions, significantly depleted of proteins, are, however, enriched in cholesterol. As a result, the choles-

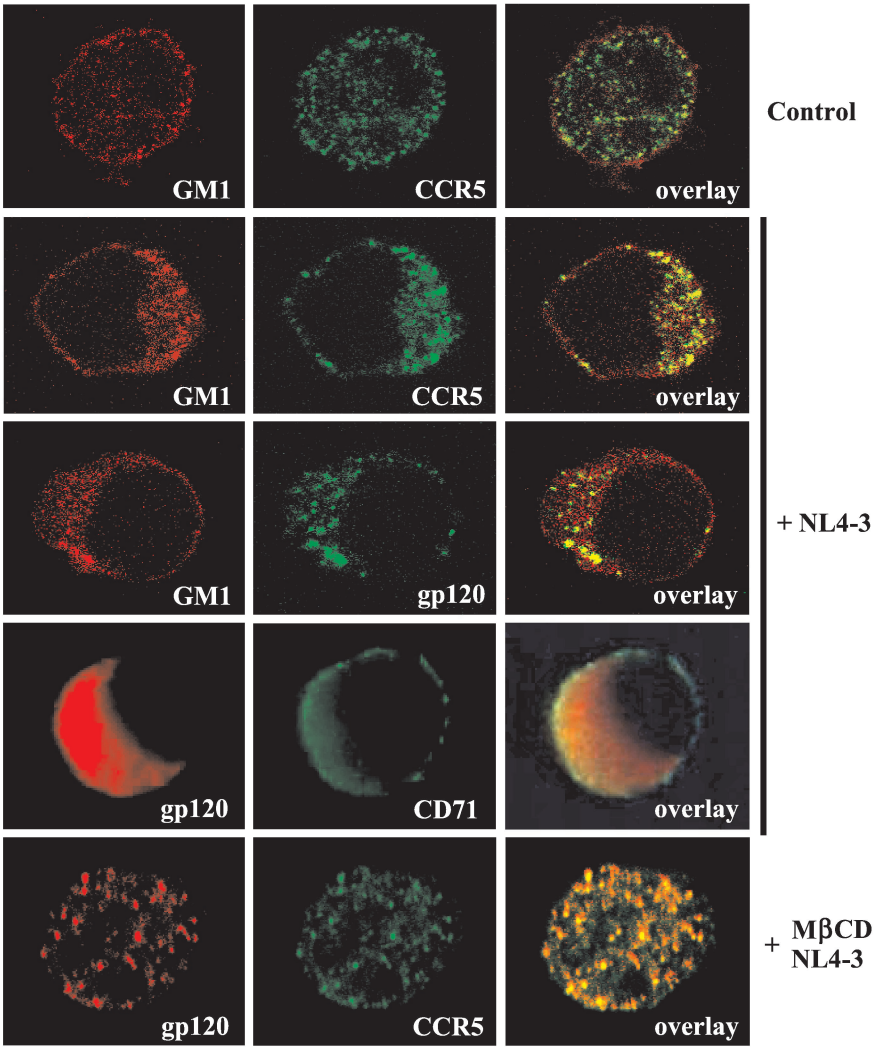

FIG. 10. HIV-1 binding to PM1 T cells triggers raft aggregation and cocapping of HIV-1 receptors. PM1 cells were incubated on ice for 30 min without (top row) or with (middle three rows) purified HIV-1 NL4-3 (5 cpm of RT/cell) and then incubated at 37°C for 45 min. (Bottom row) Alternatively, PM1 cells were first treated with 10 mM MβCD to deplete cholesterol and then infected with NL4-3. The cells were fixed with 4% paraformaldehyde and analyzed for the surface distribution of HIV-1 gp120, CCR5, the raft marker GM1, or the nonraft marker CD71. HIV-1 gp120 was visualized using FITC-conjugated monoclonal anti-gp120 (middle row) or mouse monoclonal anti-gp120 and goat anti-mouse antibodies labeled with Alexa Fluor 594 (bottom two rows). CCR5 was visualized with FITC-conjugated monoclonal anti-CCR5 (2D7) antibody. GM1 was labeled with Alexa Fluor 594 conjugates of CT-B, and CD71 was labeled with monoclonal FITC-conjugated anti-CD71 antibody.

terol/protein ratios of the detergent-resistant fractions are significantly higher than those of detergent-soluble fractions. Similar properties of erythrocyte rafts were recently documented (47). In addition, we showed that detergent-resistant fractions specifically concentrated the raft markers, ganglioside GM1 and GPI-anchored CD48, while excluding a nonraft marker, the transferrin receptor CD71 (22). These results show that detergent-resistant fractions isolated from $CD4^+$ T cells were not appreciably contaminated with proteins residing in detergent-soluble fractions. We have confirmed that membrane cholesterol is required to maintain raft integrity and extraction of plasma membrane cholesterol with MβCD relocalized raft markers into detergent-soluble fractions.

To investigate whether the integrity of lipid rafts is essential for HIV-1 entry, we analyzed, by a semiquantitative PCR, the cellular accumulation of the early reverse transcription products, R/U5, synthesized shortly after virus entry into $CD4^+$ T cells. In both Jurkat and PM1 T cells, R/U5 DNA synthesis was significantly inhibited by the depletion of membrane cholesterol with MβCD. In addition, the observed inhibition was independent of the virus tropism, as we observed the same effect with X4 NL4-3 and R5 Ad8 HIV-1. The possibility that the effect of cyclodextrin could result from potential toxicity was excluded by showing that cells exposed to MβCD and subsequently replenished with exogenous cholesterol supported virus entry (as reflected by the synthesis of R/U5 DNA) to the levels observed in untreated cells. Another possibility, that MβCD could bind to cell membranes and extract cholesterol from bound virions (36), thus destabilizing HIV-1 particles and preventing virus entry, seems less likely, since very low levels of cyclodextrin, if any, were shown to associate with cells (24). Furthermore, the observation that surface expression of

CD4 and CXCR4 receptors did not change significantly following cholesterol depletion eliminated the possibility that MβCD inhibited virus entry by downregulating these receptors. We cannot, however, exclude the possibility that extraction of cholesterol might alter the conformation of CXCR4 and its affinity for viral envelope. The existence of antigenically distinct conformations of CXCR4 has been reported (3).

Recent studies have shown that HIV-1 enters cells through receptor-mediated plasma membrane fusion, leading to productive infection, and through endocytosis, usually leading to nonproductive infection (11, 34, 48). To investigate how the depletion of cholesterol affects HIV-1 entry pathways, we used a single-cycle infectivity assay with envelope-pseudotyped virions produced by cotransfection of the luciferase gene-expressing, envelope-defective reporter construct NL4-3 Env $^{-}$LUC^{+} and vectors expressing HIV-1 HXB2 or VSV-G envelope glycoprotein. The detection of luciferase activity in cell extracts indicates successful virus entry, uncoating, reverse transcription, nuclear import, integration, and subsequent transcriptional activity. We found that viruses pseudotyped with either HXB2 or VSV-G envelopes entered the cells productively, which suggests that both receptor-mediated membrane fusion and endocytosis were functional in the cells. However, extraction of cholesterol from cell membranes resulted in 95% inhibition of luciferase activity in cells infected with virus pseudotyped with the HIV-1 envelope. In contrast, infection with virus pseudotyped with VSV envelope, which enters the cells through an endocytic pathway (1), was not inhibited following MβCD treatment. In addition, blocking the CD4 receptor with the anti-CD4 monoclonal antibody Q4120, known to compete with HIV-1 gp120 for binding, inhibited productive entry of HXB2-pseudotyped virus by 96% but did not affect infection by the virus pseudotyped with VSV-G. These results confirm that receptor-mediated and cholesterol-dependent plasma membrane fusion leads to productive infection with HIV-1. Together with results obtained in PCR-based analyses, these results suggest that raft integrity is crucial for productive entry of HIV-1.

Specific concentration of CD4 and chemokine receptors in lipid rafts may explain why HIV-1 selects these microdomains for entry. Previous studies have shown that CD4 segregates into detergent-resistant membrane microdomains (35). We have shown that CD4 and chemokine CCR5 receptors not only associate with lipid rafts but specifically concentrate in these domains to levels exceeding by severalfold their concentration in nonraft membranes. In contrast, sucrose gradient analysis revealed that the majority of CXCR4 is present in nonraft membranes. These results appear to contradict results obtained by confocal microscopy analysis showing that HIV-1 receptors colocalize significantly in membrane microdomains. However, we cannot exclude the possibility that the observed distribution of CXCR4 may result from a weak association of the receptors with rafts. It is also possible that CXCR4 receptors associate preferentially with different, Triton X-100-sensitive rafts that may also include some CD4 and CCR5 receptors. Accordingly, release of some proteins from raft domains, depending on the type and concentration of the detergent or extraction conditions used, has been reported (4, 53). Also, since multiple, distinct rafts may coexist on the cell surface (45), it is possible that some rafts may include CD4 receptors clustered separately with CXCR4 or CCR5 receptors, as was suggested recently by a study using immunogold electron microscopy (54). Alternatively, aggregation of rafts with specific anti-receptor antibodies may change the localization of raft-associated or nonraft receptors by inducing receptor-mediated signaling. These possibilities are being investigated.

The preferential association of HIV-1 gp120 envelope with lipid rafts further supports our hypothesis that HIV-1 receptors localized in these microdomains represent the population of membrane receptors engaged in virus binding and entry. How does localization of the receptors in lipid rafts affect the efficiency of HIV-1 entry and productive infection? Membrane fusion is a cooperative process (9), and it is estimated that four to six CCR5 receptors (25), multiple CD4 receptors (27), and three to six HIV-1 envelope trimers are required to form a fusion pore (10). Thus, increased concentration of these receptors in rafts will bring them into closer proximity, thereby significantly increasing the probability of forming a fusion complex and virus entry. However, this does not necessarily mean that virus fusion takes place in rafts. We speculate that virus fusion and entry may take place either in rafts or nonraft compartments, depending on virus tropism. Consequently, R5 HIV-1 may fuse in rafts due to the colocalization of CD4 with CCR5. However, for X4 HIV-1, two scenarios are possible. If CXCR4 is localized to membrane domains depleted of CD4, the CD4-HIV-1 aggregates may either leave the CD4 raft compartment, associate with CXCR4 outside rafts, and fuse with the cell membrane or stimulate entry of CXCR4 into rafts, possibly as a result of CD4-mediated signaling (41, 42). Although the nonraft receptors may play a role in virus entry through endocytic pathways, it has been suggested that these "spare" receptors may bind and transport virus particles to rafts for interaction with coreceptors and subsequent membrane fusion (12, 16).

The involvement of raft-colocalized receptors in virus entry was also suggested by the observation that HIV-1 virions bind to lipid rafts and dramatically change the pattern of raft and receptor redistribution. Intriguingly, we have observed that binding of X4 HIV-1 NL4-3 virus, known to use CD4 and CXCR4 receptors for entry, induces redistribution of CCR5 receptors. One possible explanation for these results, supported by our confocal imaging, is that CCR5 receptors colocalize with CD4 and/or CXCR4 receptors in lipid rafts. Thus, engagement of either CD4 or CXCR4 or both by HIV-1 and subsequent raft aggregation will result in clustering of CCR5 receptors.

Preferential concentration of glycosphingolipids (19) or cholesterol in lipid rafts may also affect the functional properties of the receptors and subsequent virus entry. Interestingly, it was shown that human oxytocin receptors located in cholesterol-rich membrane microdomains show higher ligand binding affinity than receptors present in cholesterol-poor microdomains (15). It is also possible that other cofactors that specifically concentrate in rafts may be required for virus entry and/or assembly and budding. For example, recent evidence suggests that lipid rafts may concentrate components of the membrane docking and fusion machinery for exocytosis (7, 26).

Importantly, entry through rafts may direct HIV-1 preintegration complexes into the correct cytoplasmic compartment. For example, it has been shown that actin may be required for

colocalization of HIV-1 receptors during entry (21) and for establishment of a functional reverse transcription complex (5). We speculate that lipid rafts may be efficiently aggregated by the stimulation of the signaling pathways emanating from these microdomains and induced by virus binding. Accordingly, rafts have been shown to be sites of the active signal-induced actin polymerization (6, 46) and stabilization of the actin cytoskeleton (13, 37).

In conclusion, we present data demonstrating the essential role of cholesterol in maintaining both lipid raft integrity and HIV-1 receptor colocalization in order to support productive virus infection. These observations could lead to the development of effective anti-HIV drug therapies that interfere with HIV-1 receptor localization in rafts and/or raft aggregation.

ACKNOWLEDGMENTS

We thank R. I. Connor for providing pNL4-3Env(−)LUC(+), D. Schols for AMD3100, and C. Broder for anti-CXCR4 monoclonal 4G10 antibody. We also thank P. M. Pitha for continued support.

This study was supported by NIH grants AI42557 and AI50461 and amfAR research grant 02766-30-RGT (W.P.).

REFERENCES

1. **Aiken, C.** 1997. Pseudotyping human immunodeficiency virus type 1 (HIV-1) by the glycoprotein of vesicular stomatitis virus targets HIV-1 entry to an endocytic pathway and suppresses both the requirement for Nef and the sensitivity to cyclosporin A. J. Virol. **71:**5871–5877.
2. **Aloia, R. C., H. Tian, and F. C. Jensen.** 1993. Lipid composition and fluidity of the human immunodeficiency virus envelope and host cell plasma membranes. Proc. Natl. Acad. Sci. USA **90:**5181–5185.
3. **Baribaud, F., T. G. Edwards, M. Sharron, A. Brelot, N. Heveker, K. Price, F. Mortari, M. Alizon, M. Tsang, and R. W. Doms.** 2001. Antigenically distinct conformations of CXCR4. J. Virol. **75:**8957–8967.
4. **Brown, D. A., and E. London.** 2000. Structure and function of sphingolipid- and cholesterol-rich membrane rafts. J. Biol. Chem. **275:**17221–17224.
5. **Bukrinskaya, A., B. Brichacek, A. Mann, and M. Stevenson.** 1998. Establishment of a functional human immunodeficiency virus type 1 (HIV-1) reverse transcription complex involves the cytoskeleton. J. Exp. Med. **188:** 2113–2125.
6. **Caroni, P.** 2001. Actin cytoskeleton regulation through modulation of $PI(4,5)P_2$ rafts. EMBO J. **20:**4332–4336.
7. **Chamberlain, L. H., R. D. Burgoyne, and G. W. Gould.** 2001. SNARE proteins are highly enriched in lipid rafts in PC12 cells: implications for the spatial control of exocytosis. Proc. Natl. Acad. Sci. USA **98:**5619–5624.
8. **Connor, R. I., K. E. Sheridan, C. Lai, L. Zhang, and D. D. Ho.** 1996. Characterization of the functional properties of *env* genes from long-term survivors of human immunodeficiency virus type 1 infection. J. Virol. **70:** 5306–5311.
9. **Doms, R. W.** 2000. Beyond receptor expression: the influence of receptor conformation, density, and affinity in HIV-1 infection. Virology **276:**229–237.
10. **Doms, R. W., and D. Trono.** 2000. The plasma membrane as a combat zone in the HIV battlefield. Genes Dev. **14:**2677–2688.
11. **Fackler, O. T., and B. M. Peterlin.** 2000. Endocytic entry of HIV-1. Curr. Biol. **10:**1005–1008.
12. **Fantini, J., D. Hammache, G. Pieroni, and N. Yahi.** 2000. Role of glycosphingolipid microdomains in CD4-dependent HIV-1 fusion. Glycoconj. J. **17:**199–204.
13. **Foger, N., R. Marhaba, and M. Zoller.** 2001. Involvement of CD44 in cytoskeleton rearrangement and raft reorganization in T cells. J. Cell Sci. **114:**1169–1178.
14. **Gatfield, J., and J. Pieters.** 2000. Essential role for cholesterol in entry of Mycobacteria into macrophages. Science **288:**1647–1651.
15. **Gimpl, G., and F. Fahrenholz.** 2000. Human oxytocin receptors in cholesterol-rich vs. cholesterol-poor microdomains of the plasma membrane. Eur. J. Biochem. **267:**2483–2497.
16. **Hammache, D., N. Yahi, M. Maresca, G. Pieroni, and J. Fantini.** 1999. Human erythrocyte glycosphingolipids as alternative cofactors for human immunodeficiency virus type 1 (HIV-1) entry: evidence for CD4-induced interactions between HIV-1 gp120 and reconstituted membrane microdomains of glycosphingolipids (Gb3 and GM3). J. Virol. **73:**5244–5248.
17. **Harder, T., and M. Kuhn.** 2000. Selective accumulation of raft-associated membrane protein LAT in T cell receptor signaling assemblies. J. Cell Biol. **151:**199–207.
18. **Hermida-Matsumoto, L., and M. D. Resh.** 2000. Localization of human immunodeficiency virus type 1 Gag and Env at the plasma membrane by confocal imaging. J. Virol. **74:**8670–8679.
19. **Hug, P., H.-M. J. Lin, T. Korte, X. Xiao, D. S. Dimitrov, J. M. Wang, A. Puri, and R. Blumenthal.** 2000. Glycosphingolipids promote entry of a broad range of human immunodeficiency virus type 1 isolates into cell lines expressing CD4, CXCR4, and/or CCR5. J. Virol. **74:**6377–6385.
20. **Iwabuchi, K., K. Handa, and S. Hakomori.** 1998. Separation of "glycosphingolipid signaling domain" from caveolin-containing membrane fraction in mouse melanoma B16 cells and its role in cell adhesion coupled with signaling. J. Biol. Chem. **273:**33766–33773.
21. **Iyengar, S., J. E. K. Hildreth, and D. H. Schwartz.** 1998. Actin-dependent receptor colocalization required for human immunodeficiency virus entry into host cells. J. Virol. **72:**5251–5255.
22. **Janes, P. W., S. C. Ley, and A. I. Magee.** 1999. Aggregation of lipid rafts accompanies signaling via the T cell antigen receptor. J. Cell Biol. **147:**447–461.
23. **Kabouridis, P. S., J. Janzen, A. L. Magee, and S. C. Ley.** 2000. Cholesterol depletion disrupts lipid rafts and modulates the activity of multiple signaling pathways in T lymphocytes. Eur. J. Immunol. **30:**954–963.
24. **Kilsdonk, E. P. C., P. G. Yancey, G. W. Stoudt, F. W. Bangerte, W. J. Johnson, M. C. Phillips, and G. H. Rothblat.** 1995. Cellular cholesterol efflux mediated by cyclodextrins. J. Biol. Chem. **270:**17250–17256.
25. **Kuhmann, S. E., E. J. Platt, S. L. Kozak, and D. Kabat.** 2000. Cooperation of multiple CCR5 coreceptors is required for infections by human immunodeficiency virus type 1. J. Virol. **74:**7005–7015.
26. **Lang, T., D. Bruns, D. Wenzel, D. Riedel, P. Holroyd, C. Thiele, and R. Jahn.** 2001. SNAREs are concentrated in cholesterol-dependent clusters that define docking and fusion sites for exocytosis. EMBO J. **20:**2202–2213.
27. **Layne, S. P., M. J. Merges, M. B. Dembo, J. L. Spouge, and P. L. Nara.** 1990. HIV requires multiple gp120 molecules for CD4-mediated infection. Nature **346:**277–279.
28. **Liao, Z., L. M. Cimakasky, R. Hampton, D. H. Nguyen, and J. E. K. Hildreth.** 2001. Lipid rafts and HIV pathogenesis: host membrane cholesterol is required for infection by HIV type 1. AIDS Res. Hum. Retrovir. **17:**1009–1019.
29. **Lu, X., and J. Silver.** 2000. Ecotropic murine leukemia virus receptor is physically associated with caveolin and membrane rafts. Virology **276:**251–258.
30. **Lu, Y. E., and M. Kielian.** 2000. Semliki Forest virus budding: assay, mechanisms, and cholesterol requirement. J. Virol. **74:**7708–7719.
31. **Lu, Y. E., T. Cassese, and M. Kielian.** 1999. The cholesterol requirement for Sindbis virus entry and exit and characterization of a spike protein region involved in cholesterol dependence. J. Virol. **73:**4272–4278.
32. **Manes, S., E. Mira, C. Gomez-Mouton, R. A. Lacalle, P. Keller, J. P. Labrador, and C. Martinez-A.** 1999. Membrane raft microdomains mediate front-rear polarity in migrating cells. EMBO J. **18:**6211–6220.
33. **Manie, S. N., S. Debreyne, S. Vincent, and D. Gerlier.** 2000. Measles virus structural components are enriched into lipid raft microdomains: a potential cellular location for virus assembly. J. Virol. **74:**305–311.
34. **Marechal, V., F. Clavel, J. M. Heard, and O. Schwartz.** 1998. Cytosolic Gag p24 as an index of productive entry of human immunodeficiency virus type 1. J. Virol. **72:**2208–2212.
35. **Millan, J., J. Cerny, V. Horejsi, and M. A. Alonso.** 1999. CD4 segregates into specific detergent-resistant T-cell membrane microdomains. Tissue Antigens **53:**33–40.
36. **Nguyen, D. H., and J. E. K. Hildreth.** 2000. Evidence for budding of human immunodeficiency virus type 1 selectively from glycolipid-enriched membrane lipid rafts. J. Virol. **74:**3264–3272.
37. **Oliferenko, S., K. Paiha, T. Harder, V. Gerke, C. Schwarzler, H. Schwarz, H. Beug, U. Gunthert, and L. A. Huber.** 1999. Analysis of CD44-containing lipid rafts: recruitment of annexin II and stabilization by the actin cytoskeleton. J. Cell Biol. **146:**843–854.
38. **Ono, A., and E. O. Freed.** 2001. Plasma membrane rafts play a critical role in HIV-1 assembly and release. Proc. Natl. Acad. Sci. USA **98:**13925–13930.
39. **Parton, R. G., and M. Lindsay.** 1999. Exploitation of major histocompatibility complex class I molecules and caveolae by simian virus 40. Immunol. Rev. **168:**23–31.
40. **Pelkmans, L., J. Kartenbeck, and A. Helenius.** 2001. Caveolar endocytosis of simian virus 40 reveals a new two-step vesicular-transport pathway to the ER. Nat. Cell Biol. **3:**473–483.
41. **Popik, W., J. E. Hesselgesser, and P. M. Pitha.** 1998. Binding of human immunodeficiency virus type 1 to CD4 and CXCR4 receptors differentially regulates expression of inflammatory genes and activates the MEK/ERK signaling pathway. J. Virol. **72:**6406–6413.
42. **Popik, W., and P. M. Pitha.** 1998. Early activation of mitogen-activated protein kinase kinase, extracellular signal-regulated kinase, p38 mitogen-activated protein kinase, and c-*Jun* N-terminal kinase in response to binding of simian immunodeficiency virus to Jurkat T cells expressing CCR5 receptor. Virology **252:**210–217.
43. **Popik, W., and P. M. Pitha.** 2000. Inhibition of CD3/CD28-mediated activation of the MEK/ERK signaling pathway represses replication of X4 but

not R5 human immunodeficiency virus type 1 in peripheral blood CD4$^+$ T lymphocytes. J. Virol. **74:**2558–2566.
44. **Pralle, A., P. Keller, E.-L. Florin, K. Simons, and J. K. H. Horber.** 2000. Sphingolipid-cholesterol rafts diffuse as small entities in the plasma membrane of mammalian cells. J. Cell Biol. **148:**997–1007.
45. **Roper, K., D. Corbeil, and W. B. Huttner.** 2000. Retention of prominin in microvilli reveals distinct cholesterol-based lipid microdomains in the apical plasma membrane. Nat. Cell Biol. **2:**582–592.
46. **Rozelle, A. L., L. M. Machesky, M. Yamamoto, M. H. E. Driessens, R. H. Insall, M. G. Roth, K. Luby-Phelps, G. Marriott, A. Hall, and H. L. Yin.** 2000. Phosphatidylinositol 4,5-bisphosphate induces actin-based movement of raft-enriched vesicles through WASP-Arp2/3. Curr. Biol. **10:**311–320.
47. **Samuel, B. U., N. Mohandas, T. Harrison, H. McManus, W. Rosse, M. Reid, and K. Haldar.** 2001. The role of cholesterol and glycosylphosphatidylinositol-anchored proteins of erythrocyte rafts in regulating raft protein content and malarial infection. J. Biol. Chem. **276:**29319–29329.
48. **Schaeffer, E., R. Geleziunas, and W. C. Greene.** 2001. Human immunodeficiency virus type 1 Nef functions at the level of virus entry by enhancing cytoplasmic delivery of virions. J. Virol. **75:**2993–3000.
49. **Scheiffele, P., M. G. Roth, and K. Simons.** 1997. Interaction of influenza virus haemagglutinin with sphingolipid-cholesterol membrane domains via its transmembrane domain. EMBO J. **16:**5501–5508.
50. **Scheiffele, P., A. Rietveld, T. Wilk, and K. Simons.** 1999. Influenza viruses select ordered lipid domains during budding from the plasma membrane. J. Biol. Chem. **274:**2038–2044.
51. **Schmidtmayerova, H., M. Alfano, G. Nuovo, and M. Bukrinsky.** 1998. Human immunodeficiency virus type 1 T-lymphotropic strains enter macrophages via a CD4- and CXCR4-mediated pathway: replication is restricted at a postentry level. J. Virol. **72:**4633–4642.
52. **Simons, K., and D. Toomre.** 2000. Lipid rafts and signal transduction. Nat. Rev. Mol. Cell Biol. **1:**31–39.
53. **Simons, K., and E. Ikonen.** 1997. Functional rafts in cell membranes. Nature **387:**569–572.
54. **Singer, I. I., S. Scott, D. W. Kawka, J. Chin, B. L. Daugherty, J. A. DeMartino, J. DiSalvo, S. L. Gould, J. E. Lineberger, L. Malkowitz, M. D. Miller, L. Mitnaul, S. J. Siciliano, M. J. Staruch, H. R. Williams, H. J. Zweerink, and M. S. Springer.** 2001. CCR5, CXCR4, and CD4 are clustered and closely apposed on microvilli of human macrophages and T cells. J. Virol. **75:**3779–3790.
55. **Xavier, R., T. Brennan, Q. Li, C. McCormack, and B. Seed.** 1998. Membrane compartmentation is required for efficient T cell activation. Immunity **8:**723–732.
56. **Xiao, X., L. Wu, T. S. Stantchev, Y. R. Feng, S. Ugolini, H. Chen, Z. Shen, J. L. Riley, C. C. Broder, Q. J. Sattentau, and D. S. Dimitrov.** 1999. Constitutive cell surface association between CD4 and CCR5. Proc. Natl. Acad. Sci. USA **96:**7496–7501.
57. **Yashiro-Ohtani, Y., X.-Y. Zhou, K. Toyo-Oka, X.-G. Tai, C.-S. Park, T. Hamaoka, R. Abe, K. Miyake, and H. Fujiwara.** 2000. Non-CD28 costimulatory molecules present in T cell rafts induce T cell costimulation by enhancing the association of TCR with rafts. J. Immunol. **164:**1251–1259.